01 Feb 1974

Eikonal Approximation Applied to Atom-Atom Excitation at Intermediate Energies: Excitation of H by H

Richard H. Shields

Jerry Peacher
Missouri University of Science and Technology, peacher@mst.edu

Eikonal approximation applied to atom-atom excitation at intermediate energies: Excitation of H by H

Richard H. Shields and Jerry L. Peacher
Physics Department, University of Missouri-Rolla, Rolla, Missouri 65401
(Received 19 July 1973)

The eikonal distorted-wave Born approximation (DWBA) developed recently by Chen, Joachain, and Watson is applied to atom-atom excitation in the intermediate energy range. In this paper the excitation of a hydrogen atom to the $2s, 2p_{\pm}$, or $2p_0$ state by hydrogen impact is considered. Differential cross sections are presented. Total cross sections are presented and compared to previous calculations. It is shown that the eikonal DWBA results for the total cross section approach the two-state distortion-approximation results in the limit of high energy and very-small-angle scattering.

I. INTRODUCTION

The eikonal distorted-wave Born approximation (DWBA) for inelastic electron-atom scattering at intermediate energies has been developed recently by Chen, Joachain, and Watson.[1] In this paper we apply their method to the analysis of inelastic H-H collisions in the intermediate-energy range.

The H-H system has been a source of extensive theoretical study. Bates and Griffing[2] in 1953 studied H-H collisions using the Born approximation in the high-energy range. Also Flannery[3] has applied the multistate impact-parameter method to H-H collisions in the intermediate-energy range. Bottcher and Flannery[4] have performed a multistate impact-parameter calculation using symmetrized atomic orbitals which enabled electron and nuclear exchange to be accounted for. Ritchie[5] has performed a two-state impact-parameter calculation in which electron exchange and the electron's translational motion were included. The present calculation will be compared to those previous results.

The eikonal DWBA, like the impact-parameter method, allows for the distortion of the incoming and outgoing plane waves. This appears as a correction factor to the plane-wave function used in the Born approximation. However, unlike the multistate impact-parameter method, both a differential and a total cross section can be calculated in the eikonal DWBA.

In Sec. II, the basic equations of the eikonal DWBA will be given, and in Sec. III, the particular matrix elements of the H-H collision will be listed. In Sec. IV, the results will be presented and the comparison of the previous results to the eikonal DWBA will be discussed.

II. BASIC EQUATIONS

The theory of the eikonal DWBA has been developed by Chen, Joachain, and Watson[1] for a general binary-rearrangement collision given by

$$A + B \rightarrow C + D. \tag{2.1}$$

We will follow their notation. In our case there is no rearrangement since we are only interested in excitation processes. Let $\vec{k}_i$ and $\vec{k}_f$ be the relative momenta[6] for the initial channel i and final channel f, respectively, for the atom-atom system in the center-of-mass coordinate system. The relative coordinate $\vec{R}$ in cylindrical coordinates, is given by

$$\vec{R} = \vec{b} + Z\hat{k}_i, \tag{2.2}$$

with b and ϕ representing the polar coordinates of $\vec{b}$ in the plane of impact parameters perpendicular to $\vec{k}_i$. Chen, Joachain, and Watson[1] assume that the interaction potential may be decomposed in the initial and final channels as (for the case of no rearrangement)

$$V = U_i + W_i \tag{2.3}$$

and

$$V = U_f + W_f. \tag{2.4}$$

A physically meaningful separation of V is to choose U_i and U_f to be functions of the relative coordinate $\vec{R}$, so that the U_i and U_f only induce elastic scattering. The natural choice is to adopt optical potentials for U_i and U_f describing elastic scattering in the initial and final channels, respectively. The U_i and U_f are incorporated into the distorted waves and the W_i (or W_f) represents that part of the interaction which induces the excitation. The T matrix in the eikonal *DWBA* for excitation from state a to state b is (in the "straight-line" approximation)

$$T_{ba}^{\text{eik}} = (2\pi)^{-3} \int_0^{\infty} db\, b \int_{-\infty}^{\infty} dZ \int_0^{2\pi} d\phi \times \exp[i(k_i - k_f \cos\theta)Z + i\delta\Phi(\vec{b}, Z) - ik_f b \sin\theta \cos\phi] A(\vec{b}, Z), \tag{2.5}$$

where θ is the angle between $\vec{k}_i$ and $\vec{k}_f$ and

$$\delta\Phi(\vec{b}, Z) = -\frac{1}{v_i}\int_{-\infty}^{Z} U_i(\vec{b}, Z')\,dZ' - \frac{1}{v_f}\int_{Z}^{\infty} U_f(\vec{b}, Z')\,dZ', \tag{2.6}$$

where v_i and v_f are the relative velocities in the initial and final channels. For excitation only (i.e., no rearrangement)

$$A(\vec{b}, Z) = \langle \psi_b|W_i|\psi_a\rangle = \langle\psi_b|W_f|\psi_a\rangle = \langle\psi_b|V|\psi_a\rangle, \tag{2.7}$$

since ψ_a and ψ_b are orthogonal and the U_i and U_f are functions of $\vec{R}$ only. The wave functions ψ_a and ψ_b are just product wave functions of the individual atoms in the initial and final channels, respectively. The differential cross section then is given by

$$\frac{d\sigma}{d\Omega} = (2\pi)^4(k_f/k_i)M^2|T_{ba}|^2, \tag{2.8}$$

where M is the reduced mass.

III. EXCITATION TO THE 2s AND 2p STATES OF HYDROGEN BY HYDROGEN IMPACT

The eikonal distorted-wave Born approximation has been applied to the process given by

$$H(1s) + H(1s) \rightarrow H(2s, 2p_{\pm}, 2p_0) + H(1s)$$

in the energy range of 2.25 keV ($v = 0.3$ a.u.) to 100 keV ($v = 2.0$ a.u.).

The interaction potential was taken as

$$V(\vec{R}, \vec{r}_{1A}, \vec{r}_{2B}) = \frac{1}{R} + \frac{1}{|\vec{R}+\vec{r}_{1A}-\vec{r}_{2B}|} - \frac{1}{|\vec{R}+\vec{r}_{1A}|} - \frac{1}{|\vec{R}-\vec{r}_{2B}|} \tag{3.1}$$

where $\vec{r}_{1A}$ and $\vec{r}_{2B}$ are the distances to the electrons from their respective nuclei.

The wave function ψ is a product of hydrogenic wave functions. For example, for the $1s \rightarrow 2s$ excitation, $\psi_a = \phi_{1s}(\vec{r}_{1A})\phi_{1s}(\vec{r}_{2B})$ and $\psi_b = \phi_{1s}(\vec{r}_{1A})\phi_{2s}(\vec{r}_{2B})$. The optical potentials are approximated by the corresponding static potentials and the elastic matrix elements are

$$U_i(\vec{R}) = \langle \phi_{1s}(\vec{r}_{1A})\phi_{1s}(\vec{r}_{2B})|V(\vec{R}, \vec{r}_{1A}, \vec{r}_{2B})|\phi_{1s}(\vec{r}_{1A})\phi_{1s}(\vec{r}_{2B})\rangle = \frac{e^{-2R}}{24}\left(\frac{24}{R}+15-18R-4R^2\right), \tag{3.2}$$

$$U_f^{2s}(\vec{R}) = \langle \phi_{1s}(\vec{r}_{1A})\phi_{2s}(\vec{r}_{2B})|V(\vec{R}, \vec{r}_{1A}, \vec{r}_{2B})|\phi_{1s}(\vec{r}_{1A})\phi_{2s}(\vec{r}_{2B})\rangle = \frac{1}{81}\left[e^{-R}\left(\frac{209}{R}-\frac{669}{4}+\frac{225R}{4}-\frac{63R^2}{8}\right)+e^{-2R}\left(-\frac{128}{R}+36\right)\right], \tag{3.3}$$

$$U_f^{2p_0}(\vec{R}) = \langle \phi_{1s}(\vec{r}_{1A})\phi_{2p_0}(\vec{r}_{2B})|V(\vec{R}, \vec{r}_{1A}, \vec{r}_{2B})|\phi_{1s}(\vec{r}_{1A})\phi_{2p_0}(\vec{r}_{2B})\rangle = U_0(R) + (3Z^2/R^2 - 1)U_2(R), \tag{3.4}$$

and

$$U_f^{2p_+}(\vec{R}) = \langle \phi_{1s}(\vec{r}_{1A})\phi_{2p_+}(\vec{r}_{2B})|V(\vec{R}, \vec{r}_{1A}, \vec{r}_{2B})|\phi_{1s}(\vec{r}_{1A})\phi_{2p_+}(\vec{r}_{2B})\rangle = U_0(R) - \tfrac{1}{2}(3Z^2/R^2 - 1)U_2(R), \tag{3.5}$$

where

$$U_0(R) = \frac{1}{1944}\left[e^{-R}\left(\frac{664}{R}-558+198R-63R^2\right)+e^{-2R}\left(\frac{1280}{R}+1824\right)\right] \tag{3.6}$$

and

$$U_2(R) = \frac{1}{1944}\left[e^{-R}\left(\frac{912}{R^3}+\frac{912}{R^2}-\frac{56}{R}-360+198R-63R^2\right)-16e^{-2R}\left(\frac{57}{R^3}+\frac{114}{R^2}+\frac{82}{R}+12\right)\right]. \tag{3.7}$$

The coupling matrix elements are given by

$$A_{2s}(\vec{R}) = \langle\phi_{1s}(\vec{r}_{1A})\phi_{2s}(\vec{r}_{2B})|V(\vec{R}, \vec{r}_{1A}, \vec{r}_{2B})|\phi_{1s}(\vec{r}_{1A})\phi_{1s}(\vec{r}_{2B})\rangle = \frac{4\sqrt{2}}{2401}\left[e^{-3R/2}\left(\frac{12288}{R}-4403+\frac{1127R}{2}\right)-e^{-2R}\left(\frac{12288}{R}+1792\right)\right], \tag{3.8}$$

$$A_{2p_0}(\vec{R}) = \langle \phi_{1s}(\vec{r}_{1A})\phi_{2p_0}(\vec{r}_{2B})|V(\vec{R}, \vec{r}_{1A}, \vec{r}_{2B})|\phi_{1s}(\vec{r}_{1A})\phi_{1s}(\vec{r}_{2B})\rangle = (Z/R)A_0(R), \tag{3.9}$$

and

$$A_{2p_+}(\vec{R}) = \langle \phi_{1s}(\vec{r}_{1A})\phi_{2p_+}(\vec{r}_{2B})|V(\vec{R}, \vec{r}_{1A}, \vec{r}_{2B})|\phi_{1s}(\vec{r}_{1A})\phi_{1s}(\vec{r}_{2B})\rangle = (-b/\sqrt{2}R)e^{i\phi}A_0(R), \tag{3.10}$$

where

$$A_0(R)=\frac{48\sqrt{2}}{2401}\left[e^{-3R/2}\left(\frac{440}{R^2}+\frac{660}{R}-273+\frac{1127R}{24}\right)-8e^{-2R}\left(\frac{55}{R^2}+\frac{110}{R}+14\right)\right]. \tag{3.11}$$

The ϕ integration in the T matrix, Eq. (2.5), can be performed and the J_0 or J_1 Bessel function will result. For example, the T-matrix element can be written for the $2s$ excitation as

$$T^{\rm eik}_{2s,\,1s}=(2\pi^2)^{-1}\int_0^\infty db\, bJ_0(bk_f\sin\theta)\,e^{i\Phi^{2s}(b)} \times\int_0^\infty A_{2s}(b,Z)\cos[(k_i-k_f\cos\theta)Z+\gamma^{2s}(b,Z)]dZ, \tag{3.12}$$

where

$$\Phi^{2s}(b)=\int_0^\infty\left(\frac{-U_i(b,Z)}{v_i}-\frac{U_f^{2s}(b,Z)}{v_f}\right)dZ \tag{3.13}$$

and

$$\gamma^{2s}(b,Z)=\int_0^Z\left(\frac{-U_i(b,Z')}{v_i}+\frac{U_f^{2s}(b,Z')}{v_f}\right)dZ'. \tag{3.14}$$

A Gaussian quadrature was used for the numerical solution of Eq. (3.12). Care was taken such that oscillations produced by the Bessel function and the factor $e^{i\Phi^{2s}(b)}$ would be followed by the numerical method. Since there are no long-range terms in the coupling matrix $A_{2s}(\vec{R})$, the oscillations die out quickly, enabling the numerical computations to converge within a reasonable amount of computation time.

IV. RESULTS AND DISCUSSION

A. Differential cross sections

In Figs. 1–3 the differential cross sections for the $1s-2s$ excitation are plotted versus the scattering angle θ for the incident velocities $v=0.3$, 0.5, and 1.0 a.u. for both the eikonal DWBA and the first Born approximation. Some general characteristics of the eikonal DWBA can be seen. One consistent observation is that the eikonal DWBA curve lies below the first-Born-approximation

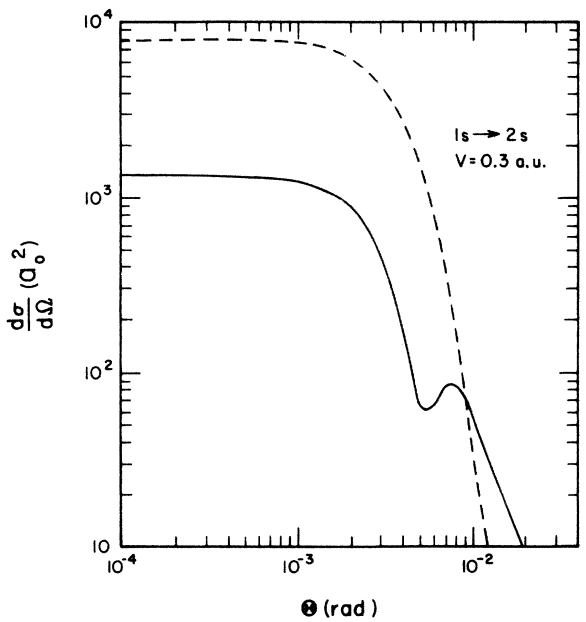

FIG. 1. Differential cross sections for the excitation of hydrogen to the $2s$ state by hydrogen impact for an incident velocity of 0.3 a.u. or for an incident energy of 2.25 keV. The solid line is the eikonal DWBA and the dashed line is the first Born approximation. Both the differential cross section and the scattering angle are given in the center-of-mass coordinate system.

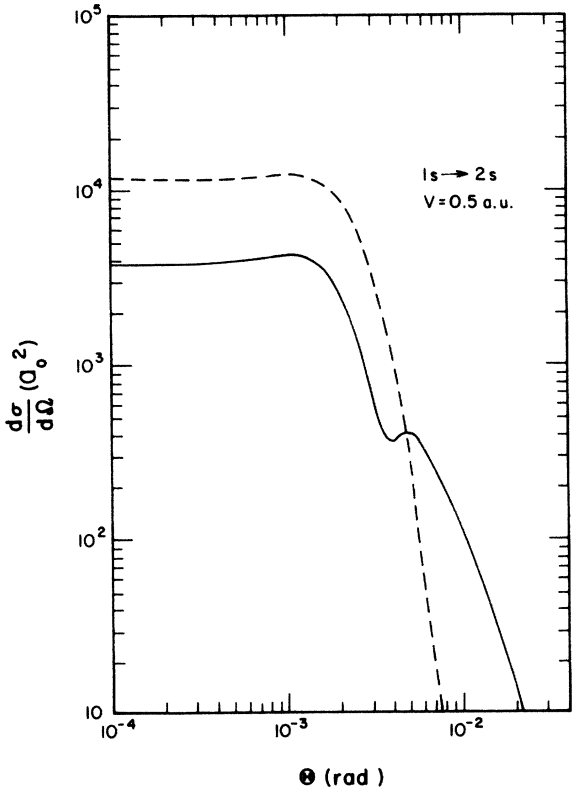

FIG. 2. Differential cross sections for the excitation of hydrogen to the $2s$ state by hydrogen impact for an incident velocity of 0.5 a.u. or for an incident energy of 6.25 keV. The solid line is the eikonal DWBA and the dashed line is the first Born approximation. Both the differential cross section and the scattering angle are given in the center-of-mass coordinate system.

curve for small angles and then crosses the Born curve and remains above it for the larger angles. The eikonal DWBA differential cross sections die off very slowly for large angles. This region of large-angle scattering becomes very important when the total cross section is calculated. For example, in Fig. 3 for $v = 1.0$ a.u., the eikonal DWBA curve falls below the Born curve for small angles and then crosses above the Born curve at a scattering angle of $\theta = 2.4 \times 10^{-3}$ rad where the differential cross section lying outside the crossing point constitutes 38% of the total cross section for the eikonal DWBA for this case ($v = 1.0$ a.u.).

Another characteristic of the eikonal DWBA differential cross sections is the second peak. The peak is quite sharp in Fig. 1 for $v = 0.3$ a.u. and flattens out for the higher velocities as shown in Figs. 2 and 3. For $v = 2.0$ a.u., the peak has disappeared and the difference between the Born and the eikonal DWBA is small.

The physical significance of the second peak is hard to determine. However, it is due to the interference between the distortion factor $e^{i\Phi(b)}$ and the Bessel function $J_m(bk_f \sin\theta)$. The result of the Z integration varies quite slowly with angle and therefore does not contribute to the second peak. The function $\Phi(b)$ behaves as $\ln b$ for small b and as $e^{-\lambda b}/\sqrt{b}$ for large b. Thus, the factor $e^{i\Phi(b)}$, which is not a function of the scattering angle, oscillates rapidly for small b and slowly for large b until asymptotically the factor equals 1. The factor $J_m(bk_f \sin\theta)$ is also an oscillating function. The product of these two factors causes the b integration to be the sum of positive and negative areas. The areas vary with angle and at a certain angle the sum of the areas creates a relative minimum in the differential cross sections and at another angle a relative maximum.

In Figs. 4–6, the differential cross sections for the $1s \rightarrow 2p_0$, $2p_\pm$ excitations are plotted versus the scattering angle for $v = 0.3, 0.5$, and 1.0 a.u. for both the eikonal DWBA and the first Born approxi-

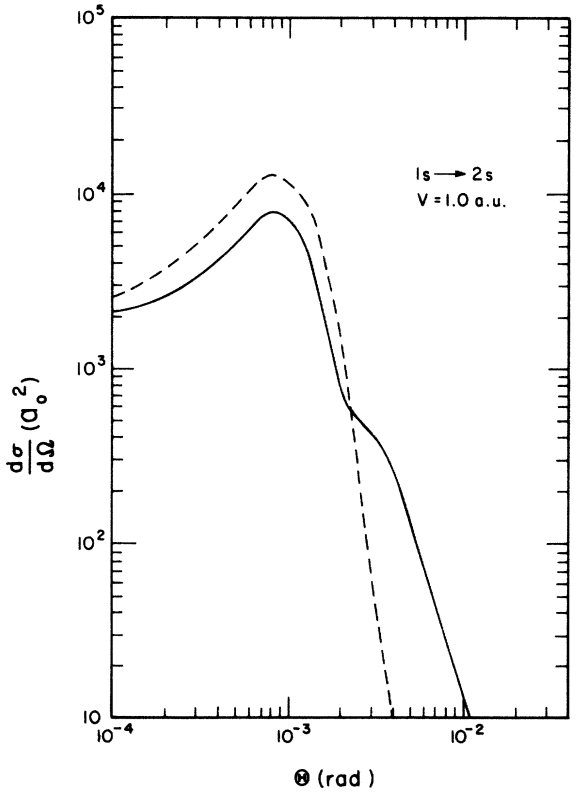

FIG. 3. Differential cross sections for the excitation of hydrogen to the $2s$ state by hydrogen impact for an incident velocity of 1.0 a.u. or for an incident energy of 25 keV. The solid line is the eikonal DWBA and the dashed line is the first Born approximation. Both the differential cross section and the scattering angle are given in the center-of-mass coordinate system.

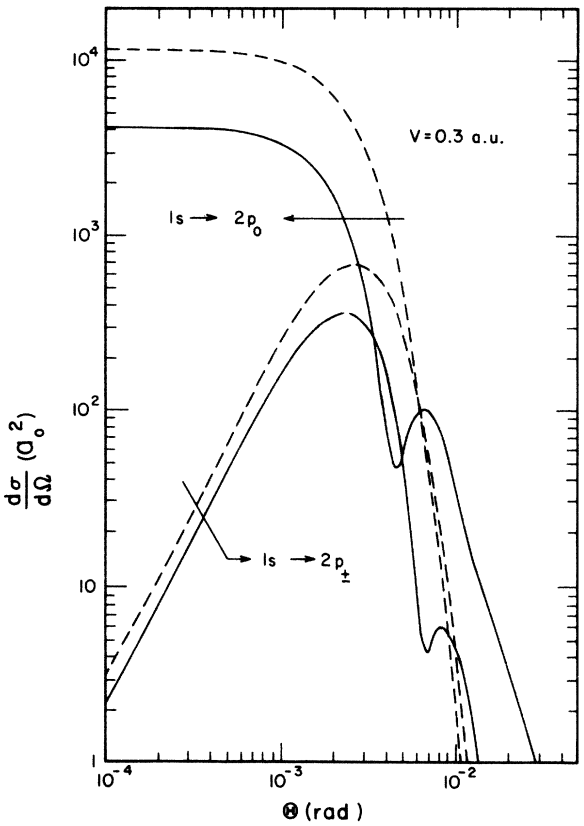

FIG. 4. Differential cross section for the excitation of hydrogen to the $2p_0$ and $2p_\pm$ states by hydrogen impact for an incident velocity of 0.3 a.u. or for an incident energy of 2.25 keV. The solid line is the eikonal DWBA and the dashed line is the first Born approximation. Both the differential cross section and the scattering angle are given in the center-of-mass coordinate system.

mation. The characteristics discussed for the $1s \rightarrow 2s$ excitation are still present. The eikonal DWBA curves are below the first-Born-approximation curves for small angles and then cross the Born curves and remain above them for the larger angles. This larger-angle scattering is important in the calculation of the total cross section from the differential cross section. For the velocity $v = 1.0$ a.u., the eikonal differential cross section for the $2p_0$ excitation crosses the Born curve at a scattering angle of $\theta = 1.3 \times 10^{-3}$ rad. Twenty-three percent of the total cross section lies outside this crossing point. The $2p_{\pm}$ excitation differential cross section has a crossing point of $\theta = 2.2 \times 10^{-3}$ rad at $v = 1.0$ a.u. and only 1% of the total cross section lies outside this region.

The second peak also occurs for the $2p_0$ and the $2p_{\pm}$ curves for the eikonal DWBA. These peaks become sharper at lower velocities as shown in Fig. 4 and then flatten out at higher velocities as shown in Figs. 5 and 6. The occurrence of these peaks is still attributed to the interference of the distortion factor $e^{i\Phi(b)}$ and the Bessel function $J_m(bk_f \sin\theta)$.

B. Total cross sections

The differential cross sections of Sec. IV A have been integrated to yield a total cross section. In Fig. 7, the total cross section for the $1s \rightarrow 2s$ excitation is presented for the eikonal DWBA, the first Born approximation, the two-state and four-state impact-parameter calculation of Flannery,[3] the impact-parameter calculation using symmetrized atomic orbitals by Bottcher and Flannery,[4] and the two-state impact-parameter calculation including electron exchange and electron translational motion by Ritchie.[5] All the methods converge to the same curve for large velocities and differ considerably at the lower velocities. However, the eikonal DWBA does seem to follow the impact-parameter calculations, especially the two-state approximation.

In Figs. 8 and 9, the total cross sections are

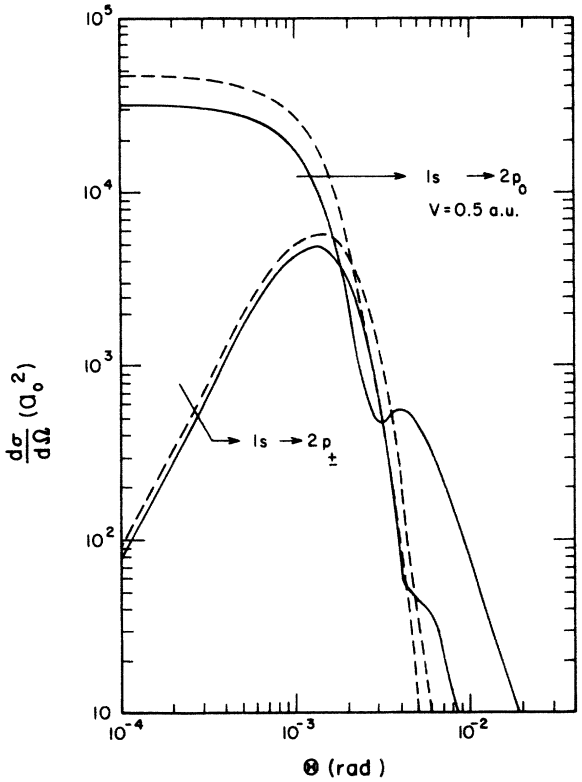

FIG. 5. Differential cross section for the excitation of hydrogen to the $2p_0$ and $2p_{\pm}$ states by hydrogen impact for an incident velocity of 0.5 a.u. or for an incident energy of 6.25 keV. The solid line is the eikonal DWBA and the dashed line is the first Born approximation. Both the differential cross section and the scattering angle are given in the center-of-mass coordinate system.

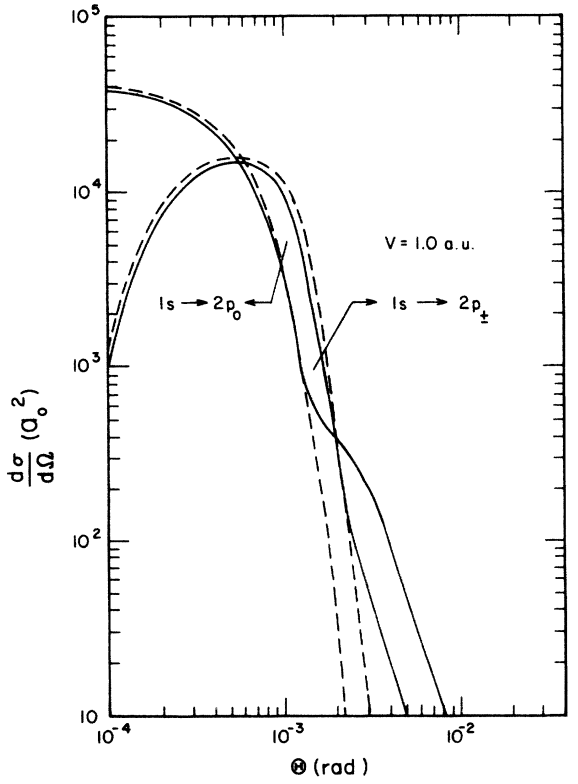

FIG. 6. Differential cross section for the excitation of hydrogen to the $2p_0$ and $2p_{\pm}$ states by hydrogen impact for an incident velocity of 1.0 a.u. or for an incident energy of 25 keV. The solid line is the eikonal DWBA and the dashed line is the first Born approximation. Both the differential cross section and the scattering angle are given in the center-of-mass coordinate system.

presented for the $2p_0$ and $2p_\pm$ excitation. The curves in these figures are the same as in Fig. 7 except that the two-state calculation of Flannery[3] has been deleted since it follows very close to the four-state curve. Also the two-state calculation of Ritchie[5] was only for the $2s$ excitation.

The closeness of the two-state impact-parameter method and the eikonal DWBA raises a question as to whether there is a relationship between the two methods. One can show that the usual two-state distortion approximation is equivalent to our approximate eikonal DWBA in the limit of high energy and very small scattering angle, namely

$$|k_i| >> (2M\Delta E)^{1/2} \tag{4.1}$$

and

$$\cos^{-1}\hat{k}_i \cdot \hat{k}_f = \theta \ll 1, \tag{4.2}$$

where ΔE is the change in kinetic energy or the electronic excitation energy. The conservation of energy equation can be approximated using Eq. (4.1) to obtain

$$k_i - k_f \simeq \Delta E/v, \tag{4.3}$$

where

$$v \simeq v_i \simeq v_f . \tag{4.4}$$

The T matrix, Eq. (2.5) can then be written as

$$T_{fi}^{\text{eik}} = (2\pi)^{-3} \int_0^{2\pi} \int_0^{\infty} b\,db\,d\phi \times \int_{-\infty}^{\infty} dZ \exp\left[\frac{i\Delta E Z}{v} + i\,\delta\Phi(b, Z) + i(\vec{k}_i - \vec{k}_f)\cdot\vec{b}\right] A(b, Z). \tag{4.5}$$

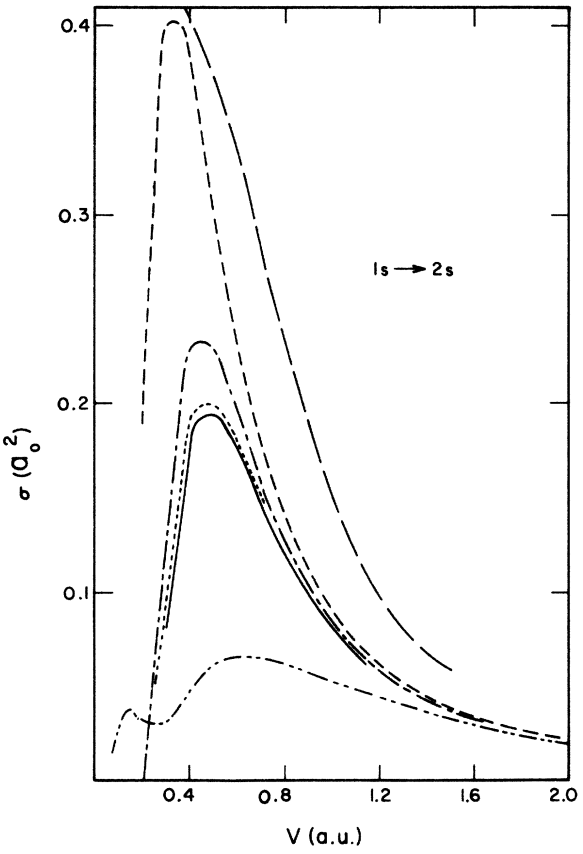

FIG. 7. Total cross section for the excitation of hydrogen to the $2s$ state by hydrogen impact. The solid line is the eikonal DWBA and the dashed line is the first Born approximation. The dash-dot line and the dotted line are the four-state and the two-state impact-parameter calculations of Flannery, Ref. 3. The dash–double-dot line is the impact-parameter calculation using symmetrized atomic orbitals by Bottcher and Flannery, Ref. 4, and the long-dash line is the two-state impact-parameter calculation, including electron exchange and the translational motion of the electrons, by Ritchie, Ref. 5.

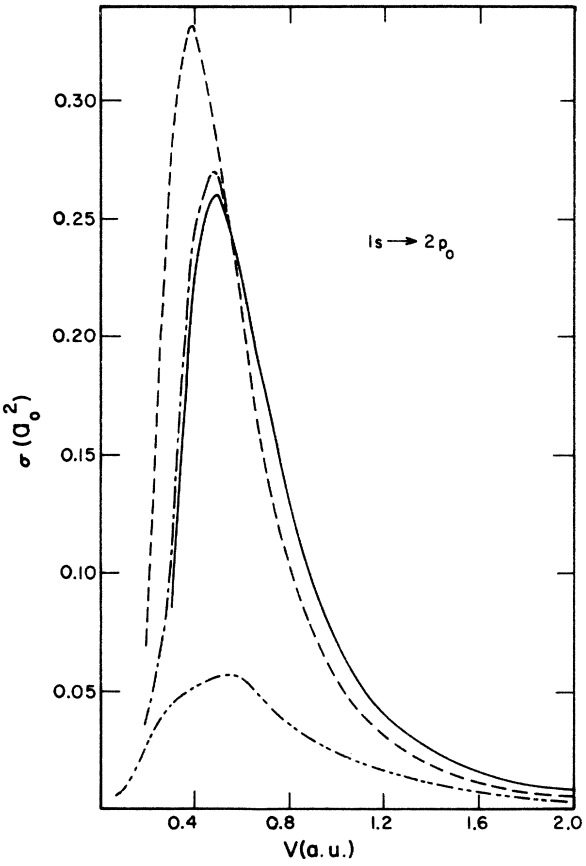

FIG. 8. Total cross section for the excitation of hydrogen to the $2p_0$ state by hydrogen impact. The solid line is the eikonal DWBA and the dashed line is the first Born approximation. The dash-dot line is the four-state impact-parameter calculation of Flannery, Ref. 3. The dash–double-dot line is the impact-parameter calculation using symmetrized atomic orbitals by Bottcher and Flannery, Ref. 4.

Using the notation introduced in Eqs. (3.13) and (3.14), the exponential factors can be written as

$$\frac{i\Delta EZ}{v} + i\delta\Phi(b, Z)$$

$$= i\Phi(b) + \frac{i}{v}\left(\Delta EZ + \int_0^Z [U_f(b, Z') - U_i(b, Z')]\, dZ'\right)$$

$$\equiv i\Phi(b) + (i/v)N_{fi}(b, Z). \tag{4.6}$$

If U_i and U_f are taken to be the elastic matrix elements as given by Eqs. (3.2) and (3.3) [or Eq. (3.4) or (3.5)], then N_{fi} is the distortion factor for the transformed transition amplitude in the two-state distortion approximation.[7] To obtain the two-state distortion approximation, the transition amplitude of the multistate impact-parameter method is transformed by using

$$C_m(Z) = a_m(Z)\exp\left(\frac{i}{v}\int_0^Z U_m(b, Z')\, dZ'\right), \tag{4.7}$$

where $Z = vt$ has been used and m labels the state. The coupled differential equations of the multistate impact-parameter method can be rewritten then as

$$\frac{dC_m(Z)}{dZ} = \frac{1}{iv}\sum_{n\neq m} C_n(Z)V_{nm}(\vec{R})\, e^{-(i/v)N_{nm}}, \tag{4.8}$$

where N_{nm} is defined by Eq. (4.6) and V_{nm} is given by

$$V_{nm}(\vec{R}) = \langle\psi_n|V|\psi_m\rangle, \tag{4.9}$$

where the ψ's and V are defined as before. Also, it may be noted that $A(b, Z)$ of Eq. (2.7) and V_{nm} are just the coupling matrix elements. Equation (4.8) can be solved in a two-state approximation to give for the final state

$$C_f(b) = \frac{1}{v}\int_{-\infty}^{\infty} dZ\, A(b, Z)\, e^{-(i/v)N_{if}}. \tag{4.10}$$

The T matrix (4.5) can be written using Eqs. (4.6), (4.10), and the momentum transfer $\vec{q} = \vec{k}_i - \vec{k}_f$,

$$T_{fi}^{\text{eik}} = (2\pi)^{-3}v\int_0^{2\pi}\int_0^{\infty} b\, db\, d\phi\, e^{i\vec{q}\cdot\vec{b}}\, e^{i\Phi(b)}\, C_f(b). \tag{4.11}$$

The total cross section then can be written as

$$\sigma_f = \int \frac{d\sigma}{d\Omega} d\Omega. \tag{4.12}$$

Using the differential cross section, Eq. (2.8), and the transformation

$$d\Omega = d^2q/k_i k_f, \tag{4.13}$$

the total cross section can be written as

$$\sigma_f = (2\pi)^{-2}\int\int d^2b\, d^2b'\, C_f(b)C_f^*(b') \times \exp[i\Phi(b) - i\Phi(b')]\int_{q_{\min}}^{q_{\max}} d^2q\, e^{i\vec{q}\cdot(\vec{b}-\vec{b}')}, \tag{4.14}$$

where

$$q_{\min} = k_i - k_f \tag{4.15}$$

and

$$q_{\max} = k_i + k_f. \tag{4.16}$$

In the limit of high energy,

$$q_{\min} \simeq 0 \tag{4.17}$$

and

$$q_{\max} \simeq \infty. \tag{4.18}$$

The q integration becomes a δ function for $\vec{b}$ and $\vec{b}'$. The cross section reduces to

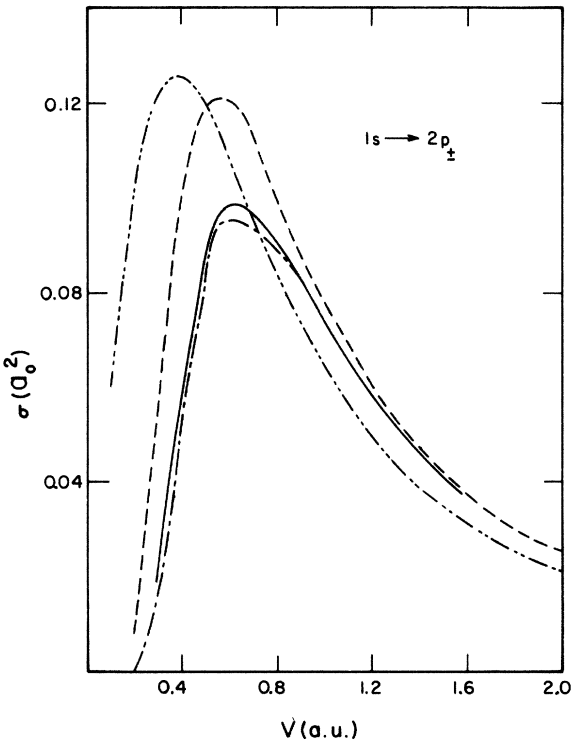

FIG. 9. Total cross section for the excitation of hydrogen to the $2p_{\pm}$ state by hydrogen impact. The solid line is the eikonal DWBA and the dashed line is the first Born approximation. The dash-dot line is the four-state impact-parameter calculation of Flannery, Ref. 3. The dash–double-dot line is the impact-parameter calculation using symmetrized atomic orbitals by Bottcher and Flannery, Ref. 4.

$$\sigma_f = \int_0^\infty d^2b\,|C_f(b)|^2 . \tag{4.19}$$

This shows that in the limits of the approximations mentioned, the eikonal DWBA and the two-state distortion approximation can be expected to yield similar results for the total cross section for very-small-angle scattering.

Electron exchange was neglected in this calculation. Bottcher and Flannery[4] have performed a calculation to determine the effect of electron exchange. They used a multistate impact-parameter approach. However, they included nuclear symmetry which is inconsistent with an impact-parameter approach. Geltman[8] has pointed out that in any impact-parameter method the assumption of a classical path forces the nuclei to be distinguishable.

Bottcher and Flannery[4] took into account the rotation of the internuclear axis during the collision. They used a standard molecular integral program that uses molecular wave functions which are all quantized along the internuclear axis and then they transformed the results to a rotating frame. The results of their calculation can be seen in Figs. 7–9. All of the cross sections are shifted from the results of Flannery's[3] impact-parameter calculation. The peaks for the $1s \rightarrow 2s$ excitation cross sections and the $1s \rightarrow 2p_0$ excitation cross sections have been lowered considerably while the peak of the $1s \rightarrow 2p_\pm$ excitation cross sections has been shifted upwards. All the results tend to the Born cross sections at the higher velocities.

Bottcher and Flannery[4] did not include a phase factor to account for the translational motion of the electron. They argued that the neglected phase factors should become more important with increasing energy. However, since their results tend to the Born cross sections at high energies, they concluded that the effect of the phase factor must be small.

Ritchie[5] has also performed a calculation to determine the effect of electron exchange. He assumed the nuclei were distinguishable for the reason mentioned above. However, he did not take into account the rotation of the internuclear axis during the collision. Instead he chose to include the translational motion of the electrons. The form of the unnormalized wave function he used was

$$\psi_n = [\,\phi_{1s}(\vec{r}_{1A})\varphi_n(\vec{r}_{2B})\,e^{-i\vec{v}'\cdot\vec{r}_1}e^{i\vec{v}'\cdot\vec{r}_2} \pm \phi_{1s}(\vec{r}_{2A})\varphi_n(\vec{r}_{1B})\,e^{i\vec{v}'\cdot\vec{r}_1}e^{-i\vec{v}'\cdot\vec{r}_2}], \tag{4.20}$$

where $\vec{r}_1$ and $\vec{r}_2$ are the distances from the center of mass to electrons 1 and 2, respectively, and $\vec{v}'$ is one half the relative velocity. The plus or minus is taken depending upon whether the spin state of the electrons is a singlet or a triplet. The phase factors are included to account for the translational motion of the electrons.

The resulting cross section can be seen in Fig. 7. The results of Ritchie[5] and the results of Bottcher and Flannery[4] show a large disagreement at all velocities. The peaks are separated by a factor of 11. This large discrepancy between the theoretical results raises some questions as to how electron exchange should be included.

Ritchie[9] in the calculation of the matrix elements makes the assumption that the velocity of the projectile is along the internuclear axis. That is, the matrix elements were calculated for a head-on collision. This greatly simplified the calculation of the matrix elements, but he assumes that the matrix elements that were calculated for a head-on collision can now be used in a two-state impact-parameter calculation in which the projectile remains at a constant impact parameter from the Z axis during the collision. His assumption that the velocity is along the internuclear axis does not allow for the rotation of the internuclear axis during the collision.

The matrix elements are a double sum due to the expansions of the plane wave $e^{i\vec{v}'\cdot\vec{r}_1}$ and the electron-electron interaction term $1/|\vec{r}_1-\vec{r}_2|$. The restriction that the velocity is along the internuclear axis enables the double sum to be reduced to a single sum. However, Ritchie's[9] assumption that the relative velocity is along the internuclear axis is unphysical since the relative velocity decreases as the impact parameter becomes larger. Also, if one uses a molecular-state basis, the rotation of the internuclear axis must be considered.

The divergent results of the two methods still raises doubts as to the importance of electron exchange in the intermediate energy range and also how electron exchange should be included since both approaches contain unphysical assumptions.

---

[1]J. C. Y. Chen, C. J. Joachain, and K. M. Watson, Phys. Rev. A 5, 2460 (1972).
[2]D. R. Bates and G. W. Griffing, Proc. Phy. Soc. Lond. A 66, 961 (1953).
[3]M. R. Flannery, Phys. Rev. 183, 231 (1969); Phys. Rev. 183, 241 (1969).
[4]C. Bottcher and M. R. Flannery, J. Phys. B 3, 1600 (1970).

[5]B. Ritchie, Phys. Rev. A 3, 656 (1971).
[6]We shall use atomic units (a.u.) throughout this paper.
[7]For a discussion of the two-state distortion approximation, see, for instance, S. Geltman, *Topics in Atomic Collision Theory* (Academic, New York, 1969), p. 196; or D. R. Bates, *Atomic and Molecular Processes*, (Academic, New York, 1962), p. 588.
[8]S. Geltman, *Topics in Atomic Collision Theory* (Academic, New York, 1969), p. 205.
[9]B. Ritchie, Phys. Rev. A 2, 759 (1970).